

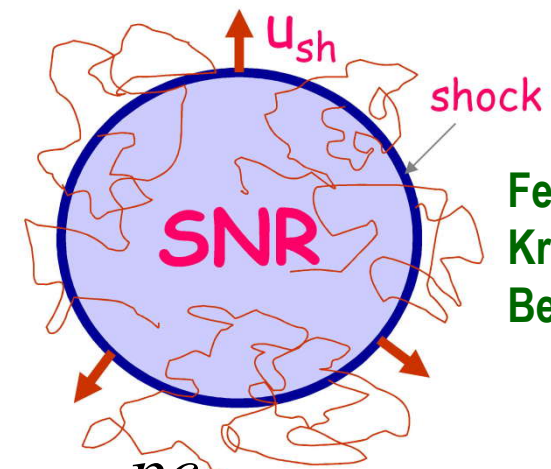
# Energy limits for acceleration of cosmic rays in supernova remnants

Vladimir Ptuskin, Vladimir Zirakashvili

*IZMIRAN, Russia*

WASDHA\_2018, Moscow

# Particle acceleration in supernova remnants: estimate of maximum energy for parallel shocks



Fermi 1949,  
Krymsky 1977,  
Bell 1978, ...

condition of acceleration  
by spherical shock

$$D \leq 0.1 V_{sh} R_{sh}$$

Bohm diffusion

$$D(p) = D_B = \frac{v r_g}{3}, \quad r_g = \frac{pc}{ZeB}$$

maximum energy

$$E_{\max} \approx 0.3 Ze \frac{V_{sh}}{c} BR_{sh}$$

observed amplified magnetic  
field in young SNRs

$$B^2 / 8\pi = f \rho V_{sh}^2, \quad f_{obs} \approx 0.035$$

$$\Rightarrow E_{\max} \approx 0.3 Z e f^{1/2} c^{-1} V_{sh}^2 R_{sh} \rho^{1/2}$$

theory of CR streaming instability gives smaller  $E_{\max}$  by factor of **~5** in the Bell's regime Bell 2004, 2012; Zirakashvili & VP 2008, Bell et al. 2013, Cardillo et al. 2015

energy achieved at the  
beginning of Sedov stage:

$$E_{\max} / Z \approx 0.2 \times \left( \frac{E_{sn}}{10^{51} \text{ erg}} \right) \left( \frac{M_{ej}}{M_{solar}} \right)^{-2/3} n^{1/6} \text{ PeV}$$

# Acceleration by perpendicular shock in wind blown bubble

development of Berezhko & Voelk (2000) model

## Stellar bubble created by powerful wind of a supernova progenitor

Weaver et al 1977

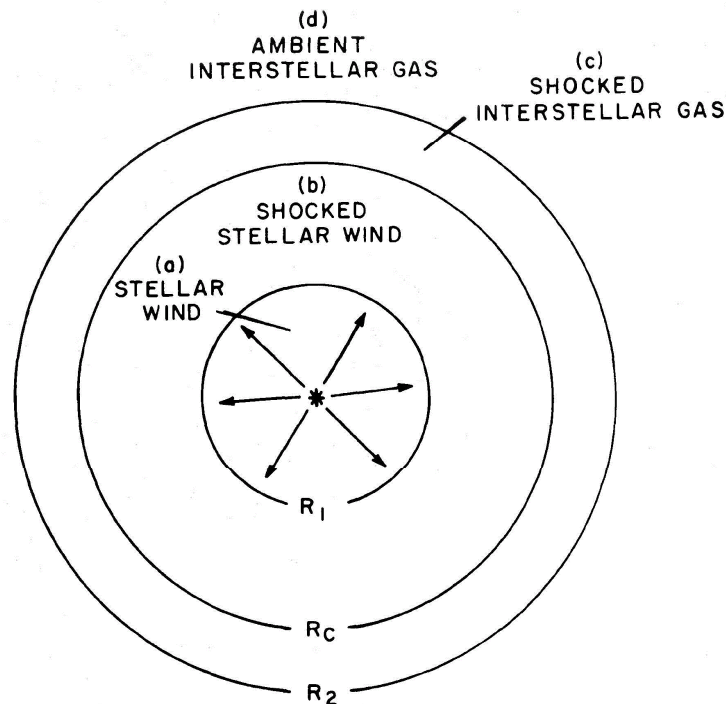


FIG. 1.—Schematic sketch indicating the regions and boundaries of the flow.

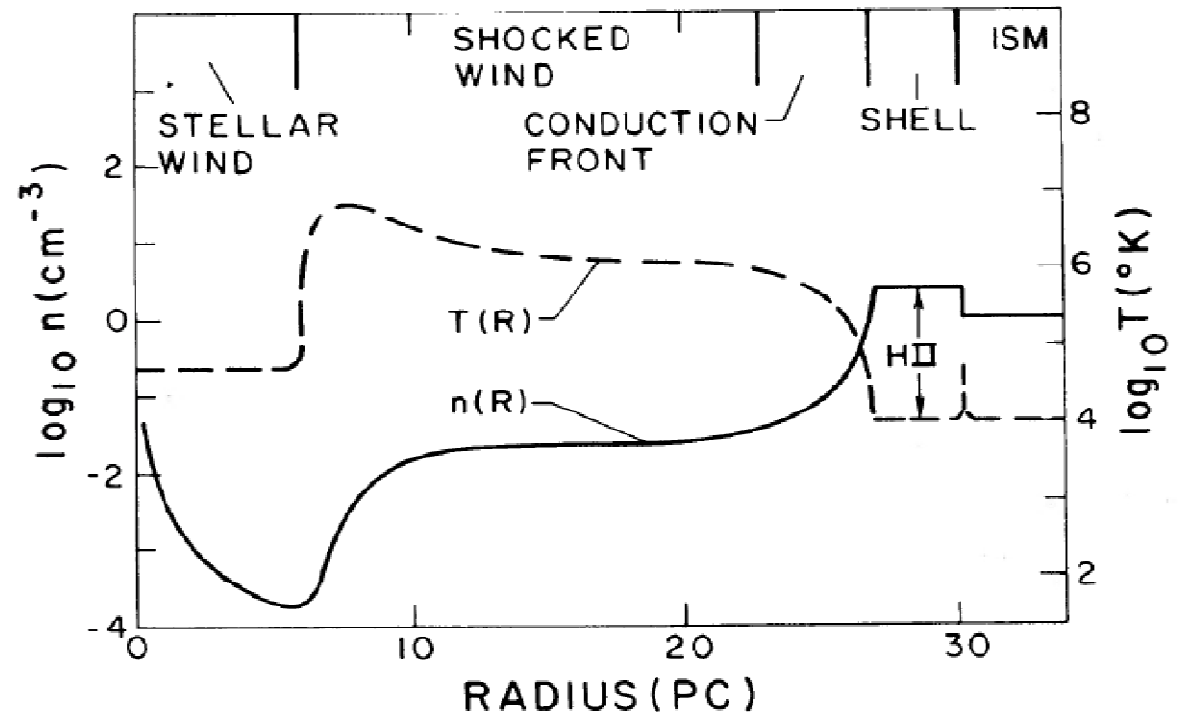
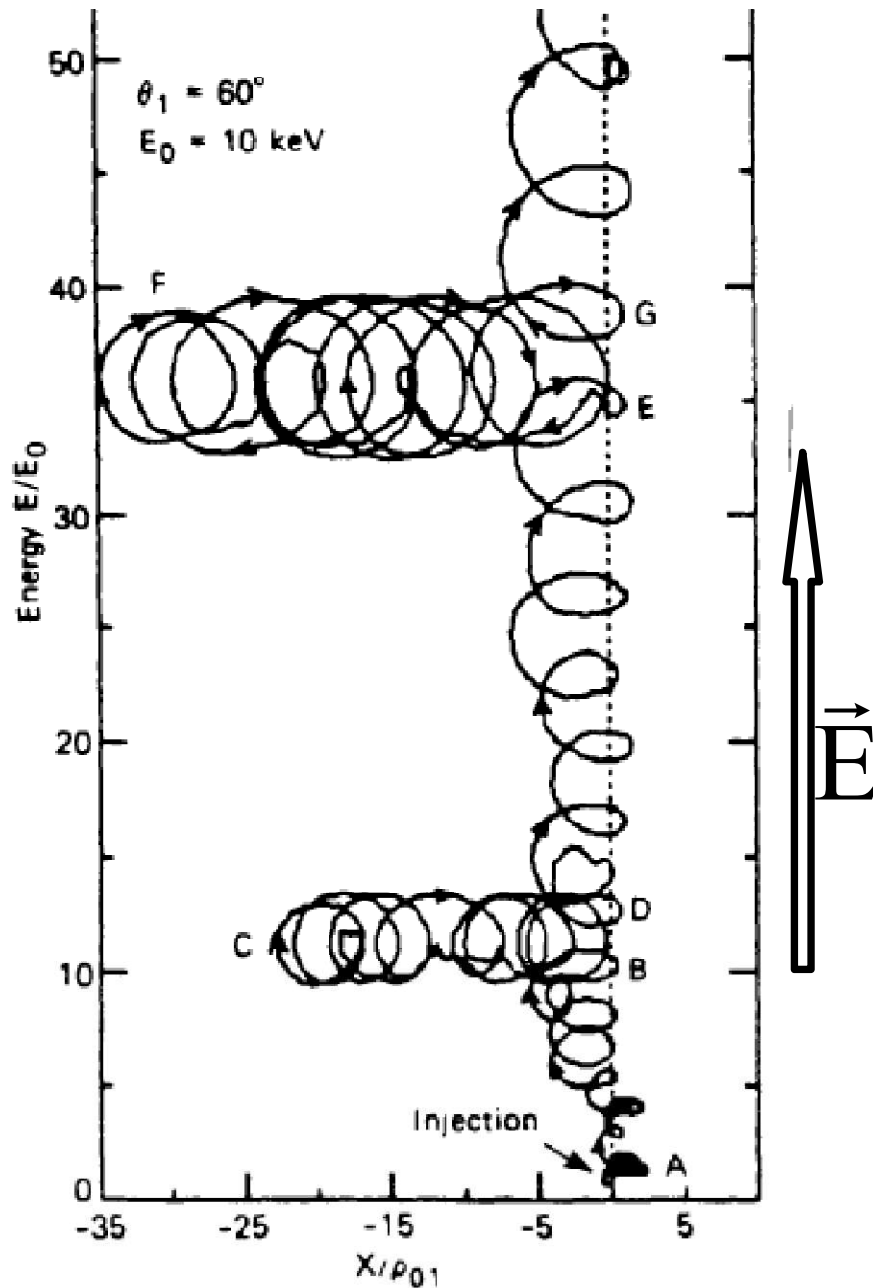


FIG. 3.—The large-scale features of the temperature and density structure of an interstellar bubble for which  $L_w = 1.27 \times 10^{36} \text{ ergs s}^{-1}$ ,  $n_0 = 1 \text{ cm}^{-3}$ , and  $t = 10^6 \text{ yr}$ . ISM means ambient interstellar medium. For a typical O7 I star, the H II region would extend to  $\sim 3 R_2$ .

# Acceleration at quasi-perpendicular shock produced by supernova explosion in star wind

Voelk, Biermann 1988, Biermann 1993, Biermann et al. 2018



Acceleration rate is high.  
Maximum particle energy is determined by electric potential difference under the condition  $|\eta| \ll 1$  where  $\eta = v/\Omega$ ,  $v$  - is scattering frequency of particles.  
No need for strong turbulence

Jokipii 1986, Takamoto, Kirk 2015, Giacalone 2017

Problem with injection

Decker, Vlahos 1985

## Maximum particle energy

$$E_{\max}^w = 3\kappa q B V_s R_s / c = \frac{3\kappa}{M_w} \frac{q V_s}{c} \sqrt{u_w \dot{M}} =$$

$$70 \text{ Z PeV} \frac{3\kappa}{M_w} \frac{V_s}{c} \left( \frac{\dot{M}}{10^{-5} M_{\odot} \text{ yr}^{-1}} \right)^{1/2} \left( \frac{u_w}{10^3 \text{ km s}^{-1}} \right)^{1/2}$$

$$\kappa \sim 0.1 \div 0.3 \quad \text{at} \quad |\eta| \leq 1$$

where  $M_w = u_w \sqrt{4\pi\rho} / B$  ( $\theta = \pi/2$ ) is wind magnetosonic Mach number

$$\longrightarrow E_{\max}^w = 0.035 \text{ PeV}$$

for Ib/c SNR with  $V_{\text{sh}} = 10^4 \text{ km/s}$ ,  $M_w = 20$ ,  $\kappa = 0.1$

### Comments:

Application to Anomalous Cosmic Rays at solar wind termination shock:

$V_s = u_w = 400 \text{ km/s}$ ,  $dM/dt = 2.5 \times 10^{-14} M_{\text{solar}} \text{ yr}^{-1}$ ,  $M_w = 20$ ,  $\kappa = 0.3$  give  $E_{\max} = 150 \text{ MeV}$ .

Acceleration at solar wind termination shock was considered by **Jokipii 1986**

# Cranfill effect: amplification of magnetic field downstream of wind termination shock (Cranfill 1971, Axford 1972, Nerney et al. 1991, Chevalier 1992)

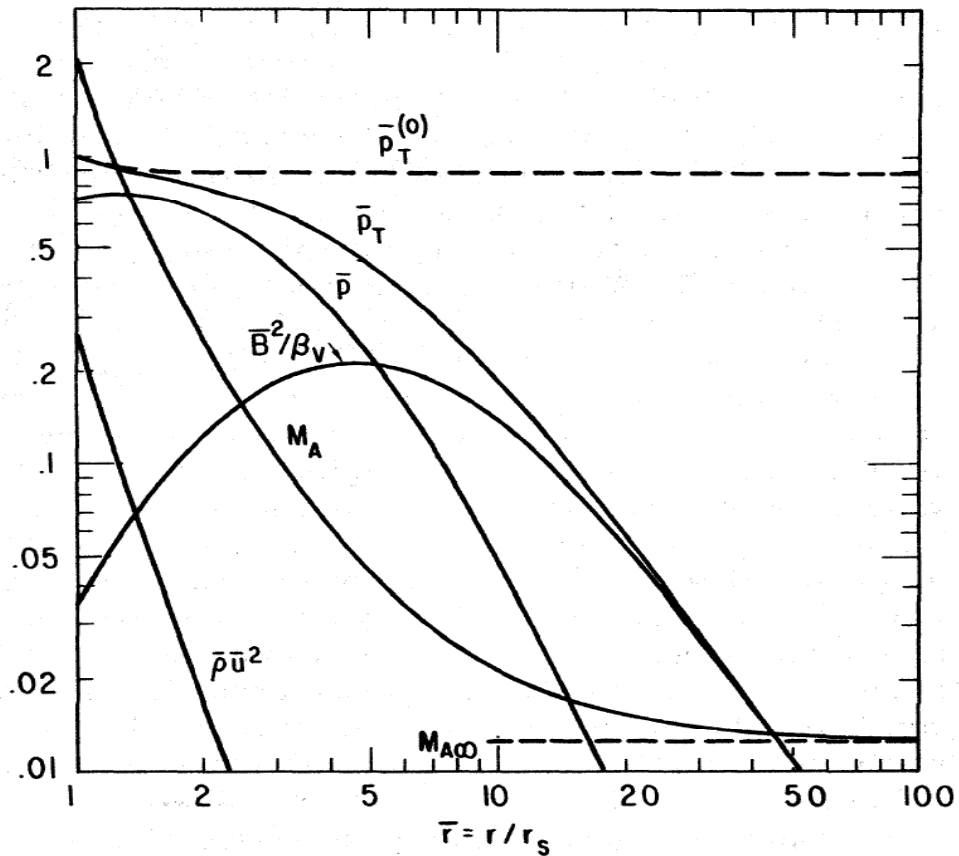


**Figure 8** Solution of equations (34)-(37) with initial conditions determined by equations (30)-(33) and with  $\beta_v = 500$ . Note that the presence of the magnetic field has caused the total pressure  $\bar{p}_T$  to decrease to zero as  $\bar{r} \rightarrow \infty$ , rather than remaining constant ( $\bar{p}_T^{(o)}$ ) as it does in the field-free case [from Cranfill, 1971].

$$\beta_v = \frac{8\pi\rho_1 v_1^2}{B_1^2}$$

energy conservation along the lines of the flow

$$\frac{u^2}{2} + \frac{\gamma}{\gamma - 1} \frac{P}{\rho} + \frac{B^2}{4\pi\rho} = \text{const}$$

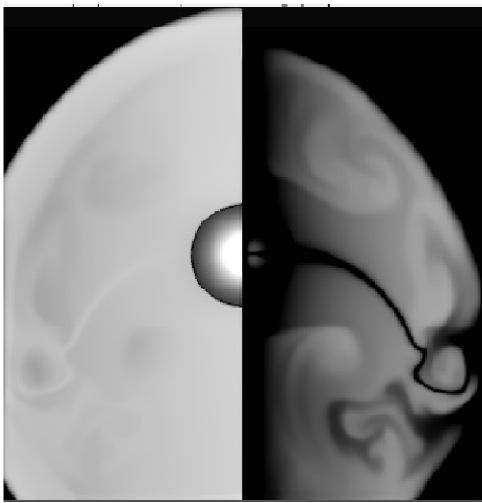


Figure 1: Gas pressure  $P_g$  (left panel) and magnetic tension  $B^2/4\pi$  (right panel) distribution in the domain  $10 \times 20$  pc at  $t = 3 \cdot 10^5$  yr. The logarithmic scaling is from  $2.3 \cdot 10^{-12}$  erg  $\text{cm}^{-3}$  (black color) to  $2.3 \cdot 10^{-10}$  erg  $\text{cm}^{-3}$  (white color). Proper stellar motion 10 km/s was taken into account.

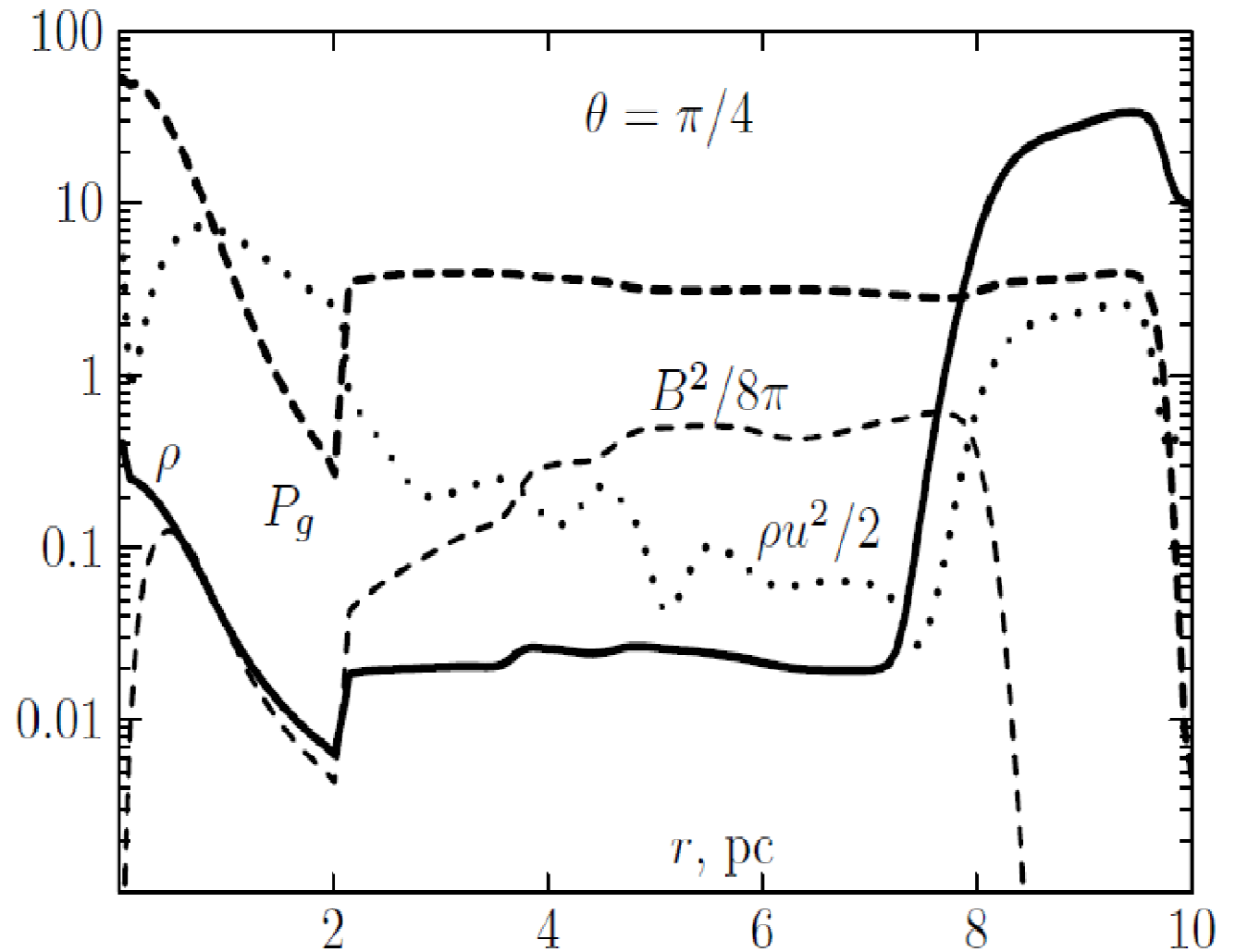
**$B \sim 20 \mu\text{G}$   
at the periphery  
if  $M_w = 20$ ,  $t \sim 300$  kyr**

## 2D MHD modeling of WR bubble

Zirakashvili, Ptuskin 2018

$$\dot{M} = 10^{-5} M_{\odot} \text{yr}^{-1}$$

$$u_w = 1000 \text{ km/s}, M_w = 20, t = 300 \text{ kyr}, n_0 = 10 \text{ cm}^{-3}$$



# Particle transport and acceleration

see details in

V.N. Zirakashvili, V.S. Ptuskin, 2018,  
Astroparticle Physics 98, 21

## Transport equation

- azimuth symmetry,
- radial flow,
- circular average magnetic field

$$\frac{\partial N}{\partial t} - \nabla D_{\perp} d \nabla N + (\mathbf{u} + \mathbf{u}_d) \nabla N - \frac{\nabla \mathbf{u}}{3} p \frac{\partial N}{\partial p} = Q$$

$$\mathbf{u}_d = [\nabla \times D_A \mathbf{b}] \quad \text{- drift velocity}$$

Variables:

$$\xi = r/R_s(t), \vartheta, \quad \frac{\partial}{\partial \varphi} = 0,$$

$$\tau = \ln(R_s(t)/R_0)$$

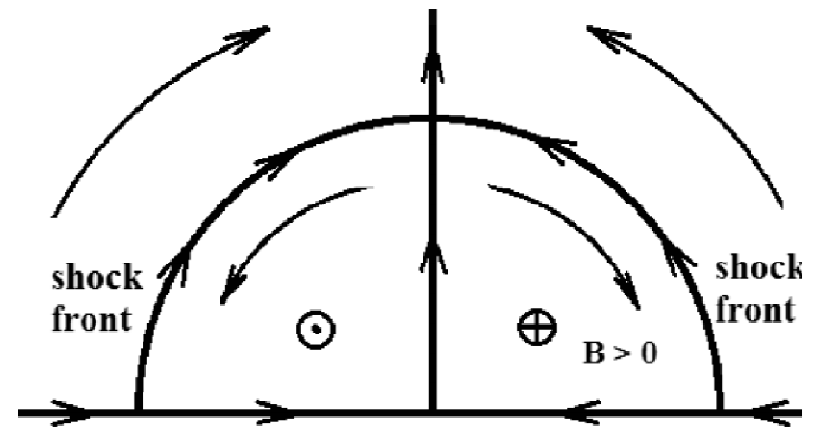


Figure 3: Drift motions of the protons accelerated at the shock propagating in the stellar wind.

Parallel diffusion coefficient

$$D_{\parallel} = \frac{v^2}{3v} \quad \text{is not important}$$

Perpendicular diffusion coefficient:

$$D_{\perp} = D_B |\eta| / (1 + \eta^2)$$

$$\eta = \nu / \Omega$$

Antisymmetric (Hall) diffusion coefficient:

$$D_A = D_{\perp} \frac{|\Omega|}{v}$$

Particle spectra  
at the shock

scattering

$$\eta = v / \Omega$$

gyrofrequency

Spatial distribution  
at the shock

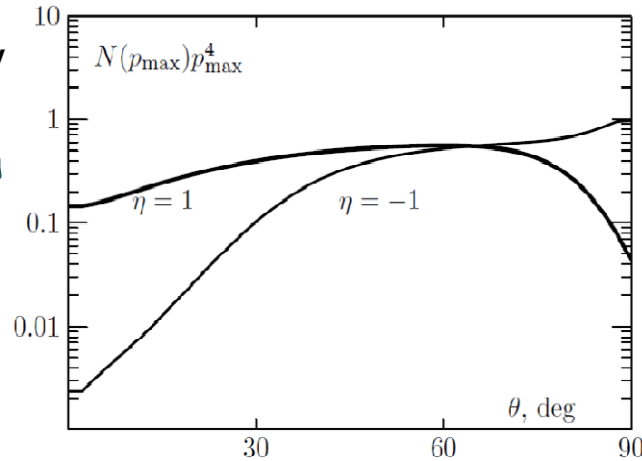
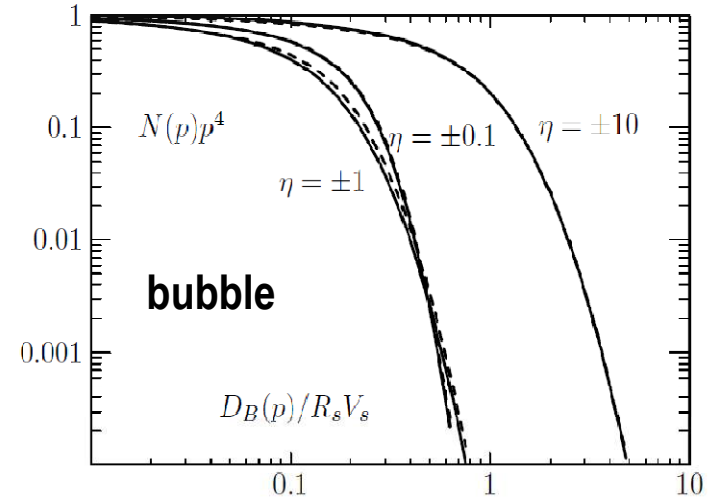
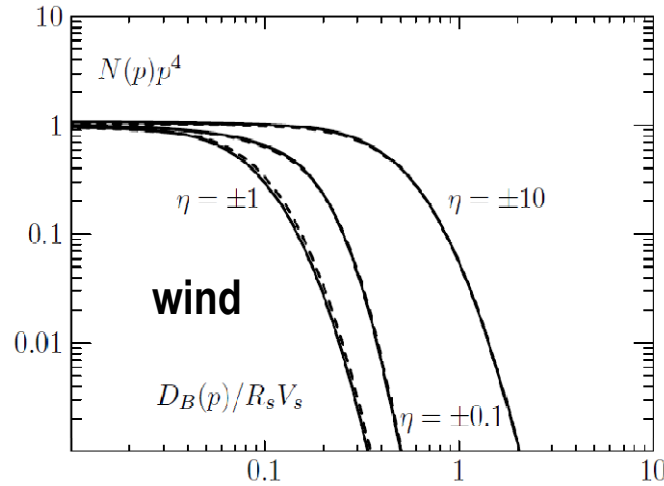


Table 1: Values of  $\kappa$  for different values of  $\eta$

$\eta$	$\pm 0.01$	$\pm 0.1$	-1.0	1.0	-10	10
wind	0.18	0.14	0.10	0.09	0.59	0.58
bubble	0.18	0.15	0.09	0.08	0.48	0.48

maximum energy of particles accelerated in bubble

$$E_{\max}^b \sim E_{\max}^w \times \frac{\sigma_{\text{TS}} R_s^2}{R_{\text{TS}}^2};$$

calculated value  $E_{\max}^b / Z = 2 \text{ PeV}$  for Ib/c SNR at age  $t_{\text{sn}} \sim 10^3 \text{ yr}$

# Discussion and conclusions

## Diversity of cosmic ray source spectra:

Estimated maximum energy of accelerated particles is close to 0.1 Pev for major part of Type IIP SNRs and several times more for Ia SNRs. Less frequent Ib/c, IIn, IIb SNRs may accelerate particles to PeV energies.

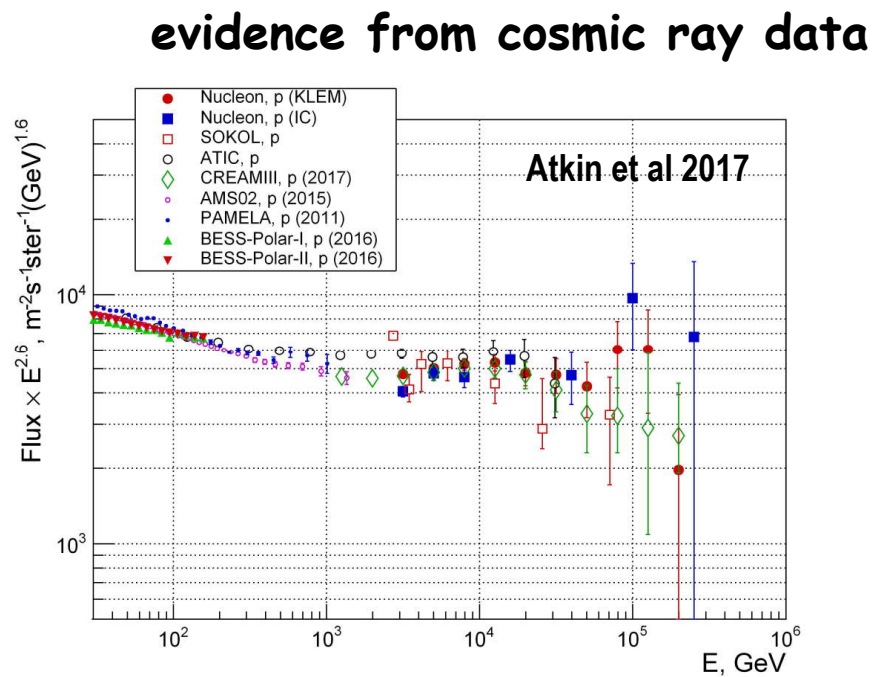


**Figure 14.** Proton spectrum measured in the NUCLEON experiment together with the data from other experiments: Sokol [14, 28], ATIC [7]; CREAM-III [8]; AMS-02 [6]; PAMELA [5]; BESS-Polar I and II [30].

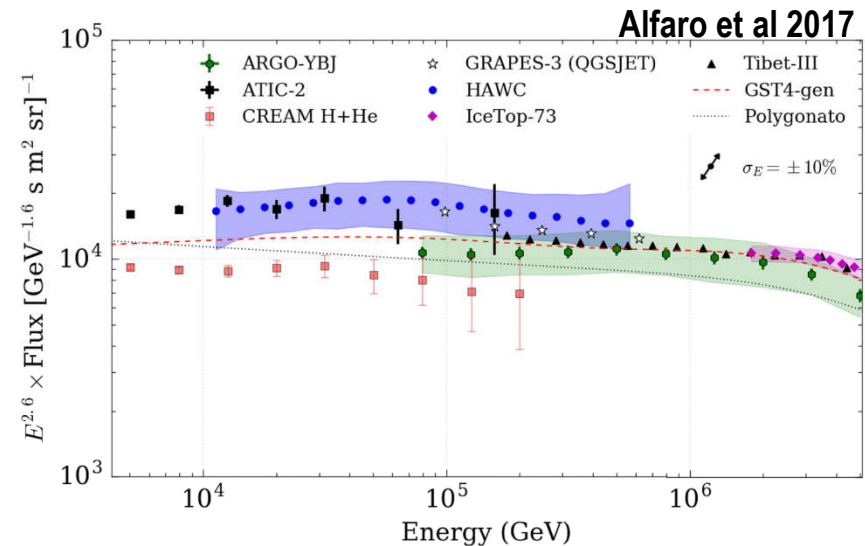


**FIG. 10.** The differential all-particle energy spectrum measured by HAWC (blue) compared with the spectra from the ARGO-YBJ [11], ATIC-2 [7], GRAPES-3 [12], IceTop [38], and Tibet-III [13] experiments. The CREAM [6] light component spectrum (H+He) is also included for comparison. The uncertainties on the ATIC-2 and CREAM measurements represent combined statistical and systematic uncertainties. For the HAWC, ARGO-YBJ, and IceTop spectra, the shaded regions represent the reported systematic uncertainties. Only ARGO-YBJ reports statistical uncertainties that are shown by visible vertical bars, while for the remaining air-shower array measurements, these are smaller than the respective marker size. The double-sided arrow indicates the shift in flux that would result from a  $\pm 10\%$  shift in the energy scale. The GST4-gen [39] and Polygonato [40] all-particle flux models are shown by the red and black dashed lines, respectively.

## Cosmic ray acceleration in magnetic circumstellar bubbles:

Bubbles produced by O and WR stars with magnetic field amplified by Cranfill effect are ideally suited for particle acceleration by quasi-perpendicular shocks. No strong cosmic-ray streaming instability is required.

Helium dominated composition is expected at the knee in the case of acceleration in WR bubbles.

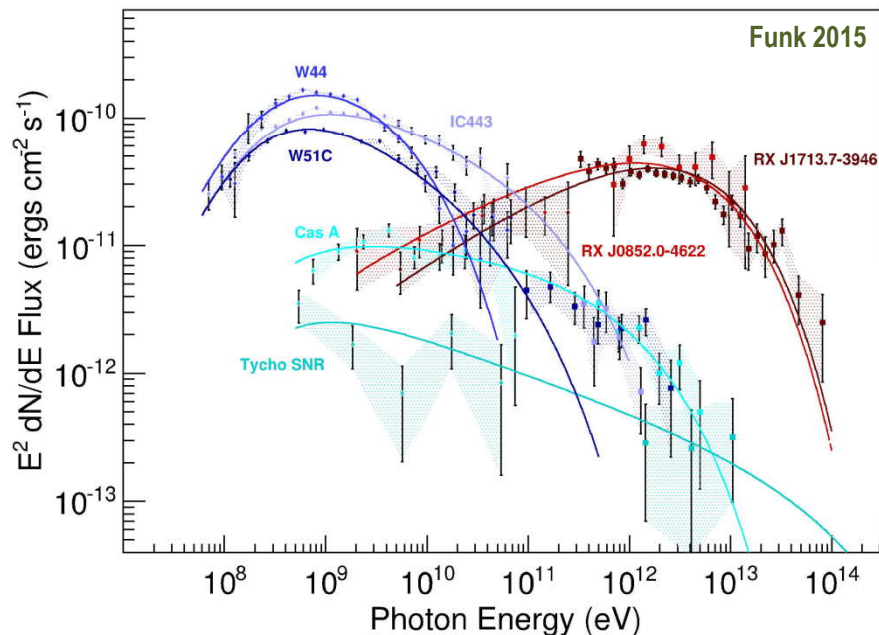
Quasiperpendicular geometry and low gas density are in favor of leptonic origin of gamma-ray emission. Hadronic mechanism probably dominates when the shock reaches dense envelope.

Several Pevatrons in Ib/c SNRs with age  $\sim 1000$  yrs may exist in the Galaxy.

## On the whole:

Two kinds of young SNRs as cosmic ray sources exists:

- SNRs where the turbulence needed for efficient shock acceleration is generated by cosmic-ray streaming instability (SN 1006, Tycho, Cas A). Maximum energy of accelerated particles is  $\sim 100$  TeV;
- SNRs in the wind blown bubbles with background turbulence and magnetic field amplified by Cranfill effect (RX J1713.7-3946, RCW 86, Vela Jr.). Acceleration by quasi-perpendicular shock allows to reach PeV energies.



Typical gamma-ray energy spectra for several of the most prominent SNRs. Young SNRs ( $< 1000$  years) are shown in cyan. These typically show smaller gamma-ray fluxes but rather hard spectra in the GeV and TeV band. The older (but still so-called young) shell-type SNRs RX J1713.7-3946 and RX J0852.0-4622 (Vela Junior) of ages  $\sim 2000$  years are shown in red colors. These show very hard spectra in the GeV band ( $\Gamma = 1.5$  and a peak in the TeV band with an exponential cutoff beyond 10 TeV). The mid-aged SNRs ( $\sim 20,000$  years) interacting with molecular clouds (W44, W51C and IC443) are shown in blue. Also shown are hadronic fits to the data (solid lines).